

Amphicarpic development in *Cardamine chenopodiifolia*

Aurélia Emonet¹ , Miguel Pérez-Antón¹ , Ulla Neumann¹ , Sonja Dunemann¹, Bruno Huettel¹ , Robert Koller²  and Angela Hay¹ 

¹Max Planck Institute for Plant Breeding Research, Carl-von-Linné-Weg 10, Köln, 50829, Germany; ²Forschungszentrum Jülich GmbH, Institute of Bio- and Geosciences, IBG-2: Plant Sciences, Wilhelm-Johnen-Street, Jülich, 52425, Germany

Summary

Author for correspondence:

Angela Hay

Email: hay@mpipz.mpg.de

Received: 19 February 2024

Accepted: 25 June 2024

New Phytologist (2024)

doi: 10.1111/nph.19965

Key words: amphicarp, *Cardamine chenopodiifolia*, comparative development, explosive seed dispersal, fruit development, lignin patterning, polyploidy.

- Amphicarp is an unusual trait where two fruit types develop on the same plant: one above and the other belowground. This trait is not found in conventional model species. Therefore, its development and molecular genetics remain under-studied. Here, we establish the allooctoploid *Cardamine chenopodiifolia* as an emerging experimental system to study amphicarp.
- We characterized *C. chenopodiifolia* development, focusing on differences in morphology and cell wall histochemistry between above- and belowground fruit. We generated a reference transcriptome with PacBio full-length transcript sequencing and analysed differential gene expression between above- and belowground fruit valves.
- *Cardamine chenopodiifolia* has two contrasting modes of seed dispersal. The main shoot fails to bolt and initiates floral primordia that grow underground where they self-pollinate and set seed. By contrast, axillary shoots bolt and develop exploding seed pods aboveground. Morphological differences between aerial explosive fruit and subterranean nonexplosive fruit were reflected in a large number of differentially regulated genes involved in photosynthesis, secondary cell wall formation and defence responses.
- Tools established in *C. chenopodiifolia*, such as a reference transcriptome, draft genome assembly and stable plant transformation, pave the way to study amphicarp and trait evolution via allopolyploidy.

Introduction

Seed dispersal strategies vary widely between different plants. In flowering plants, seeds are encased in fruit for protection and dispersal, and fruit diversity reflects the many different adaptations for dispersal found in nature. Fruit of the model plant *Arabidopsis* are dry siliques that open by dehiscence and seeds are released once the fruit structure falls apart (Dinnyen *et al.*, 2005). Genetic tools in *Arabidopsis* have been immensely useful for studying fruit development and the tissue patterning required for dehiscence (Ferrández *et al.*, 2000; Liljegren *et al.*, 2000, 2004). However, only a fraction of the diverse seed dispersal strategies found in nature are accessible through the study of model organisms.

Comparative approaches extend the reach of developmental genetics by developing new tools in less well-studied species. For example, *Cardamine hirsuta* is a relative of *Arabidopsis* with many divergent traits and genetic tools to study them (Hay & Tsiantis, 2006; Hay *et al.*, 2014; Vlad *et al.*, 2014; Monniaux *et al.*, 2018; Kierzkowski *et al.*, 2019; Baumgarten *et al.*, 2023). Explosive seed dispersal is one such trait that distinguishes *C. hirsuta* from *Arabidopsis*. Seeds are launched at speeds $> 10 \text{ ms}^{-1}$ by the explosive coiling of *C. hirsuta* fruit valves (Hofhuis *et al.*, 2016). This rapid movement spreads seeds across a large area, which is an efficient dispersal strategy for a ruderal weed.

Explosive seed dispersal is a derived trait, shared by *Cardamine* species in the Brassicaceae. A novel pattern of lignified secondary

cell walls evolved in strict association with this trait (Hofhuis *et al.*, 2016). In *Arabidopsis* and other Brassicaceae species with nonexplosive fruit, an inner layer of the fruit valve, called the endocarp *b*, is formed by cells with uniformly lignified secondary cell walls (Spence *et al.*, 1996; Hofhuis *et al.*, 2016). By contrast, this same cell wall is deposited in a distinctive polar pattern in *Cardamine* species with explosive fruit (Hofhuis *et al.*, 2016). Genetics and mathematical modelling in *C. hirsuta* have shown that this polar pattern of lignin deposition provides a mechanism to rapidly release built-up tension in the valves via explosive coiling (Hofhuis *et al.*, 2016; Pérez Antón *et al.*, 2022).

Seed dispersal strategies can also vary within a single plant through the development of two or more fruit/seed morphs. This heteromorphy is exhibited by hundreds of flowering plant species and often described as a bet-hedging strategy (Imbert, 2002; Giannela *et al.*, 2021). Plants ‘hedge their bets’ by following more than one dispersal strategy to increase their chances of success in variable environments. In the Brassicaceae, for example, *Diptychocarpus strictus* and *Aethionema arabicum* develop both dehiscent and indehiscent fruit on the same plant (Lu *et al.*, 2010, 2015; Lenser *et al.*, 2016). The dehiscent fruit in *Aethionema arabicum* release mucilaginous seeds that germinate quickly, while indehiscent fruit each produce a single seed that is not released and has delayed germination (Lenser *et al.*, 2016).

Amphicarp is a specific type of heteromorphy where one fruit morph is buried underground. Underground fruit, or geocarp, is a

strategy used by a number of species for seed dispersal, such as the agronomically important peanut plant (*Arachis hypogaea*, Zhuang *et al.*, 2019). In contrast to this, amphicarp is a dual strategy, combining the advantages of both aerial and subterranean fruit for seed dispersal (Cheplick, 1987). Amphicarp is a rare trait that evolved independently in different groups of flowering plants, particularly in the Fabaceae family (Kaul *et al.*, 2000; Zhang *et al.*, 2020; Liu *et al.*, 2021). For example, the legume *Amphicarpaea edgeworthii* is an amphicarpic plant with a sequenced genome (Liu *et al.*, 2021). Within the Brassicaceae family, one amphicarpic species belongs to the *Cardamine* genus. *Cardamine chenopodiifolia* is an annual plant, native to South America, that is easily cultivated in glasshouse conditions (Persoon, 1807; Gorczyński, 1930; Cabrera, 1967; Cheplick, 1983). A recent chromosome-level genome assembly indicates that *C. chenopodiifolia* is allooctoploid, comprising four sub-genomes of eight chromosomes each (Emonet *et al.*, 2024).

Polyploidy, or whole-genome duplication, is a common evolutionary process (Soltis *et al.*, 2016). Most diploid organisms have polyploid ancestors and about one third of plant species are examples of recent polyploidization (Van de Peer *et al.*, 2017). *Cardamine chenopodiifolia* is a naturally occurring allopolyploid, derived from the hybridization of different species (Manton, 1932; Emonet *et al.*, 2024). Many crop species are also polyploid, suggesting that the rapid genetic and genomic changes associated with whole-genome duplication may confer advantages for trait evolution (Van de Peer *et al.*, 2021). However, many trait novelties, such as amphicarp, are under-studied because the complexity of polyploid genomes makes it difficult to link genotype to phenotype with functional studies.

An interesting feature of amphicarpic development in *C. chenopodiifolia* is that it combines both explosive and nonexplosive seed dispersal. It partitions these two very different modes of seed dispersal between explosive aerial fruit and nonexplosive subterranean fruit. Comparing both traits within the same plant provides a complementary approach to comparisons between *Arabidopsis* and *C. hirsuta*. In particular, comparative transcriptomics between two fruit morphs encoded by a single genome, bypasses many of the challenges inherent to between-species comparisons. For these reasons, we characterized amphicarpic development in *C. chenopodiifolia*, focusing on the differences in morphology, cell wall histochemistry and gene expression profiles that differentiate aerial and subterranean fruit. This work establishes resources in *C. chenopodiifolia* as an emerging experimental system and identifies differences in secondary wall deposition in the fruit endocarp between the two fruit types as important determinants of explosive vs nonexplosive seed dispersal.

Materials and Methods

Plant and growth conditions

Cardamine chenopodiifolia Pers. seeds (Ipen: XX-0-MJG-19-35 600) were obtained from the Botanic Garden of the Johannes Gutenberg University, Mainz, Germany. To improve germination, aerial seeds were germinated in long days on ½ Murashige and Skoog (MS) plates after 7 d stratification, then 1-wk-old seedlings were transferred to soil and grown in long-day

(16 h : 8 h, light : dark, 20°C : 18°C; 65% humidity) or short-day conditions (8 h : 16 h, light : dark, 20°C : 18°C, 65% humidity). For magnetic resonance imaging (MRI), seedlings were transferred to Speyer 2.1 soil (loamy sand, sieved to 2 mm, brand name Sp2.1, Landwirtschaftliche Untersuchungs- und Forschungsanstalt Speyer, Speyer, Germany) and grown in a glasshouse under long-day conditions.

Plant transformation

DR5v2::NLS-tdTomato construct in a modified pPZP200 vector (Bhatia *et al.*, 2023) was transformed into *C. chenopodiifolia* by floral dip (Clough & Bent, 1998). Eighty plants were transformed, and T1 transformants were selected with basta treatment.

Seed, fruit and plant phenotyping and staging

Forty plants were grown over a period of 6 wk, and their characteristics monitored every 1 or 2 d (see Supporting Information Methods S1 for details). At 44–53 d postgermination (dpg), 17 plants were used to count aerial and subterranean fruit, measure fruit width and length, and ascribe fruit stages. A MARVIN seed counter was used to count and measure seed weight and dimensions of dry aerial and subterranean seeds from 4 plants.

Mucilage assay

Seed mucilage was stained with 0.01% ruthenium red solution (McFarlane *et al.*, 2014) and imaged under a Niko SMZ18 binocular with SHR Plan Apo 1.6× WD30 objective.

Photography

Photographs of plants at different stages were taken with a Nikon D800 equipped with either AF-S Micro NIKKOR 105 mm 1 : 2.8 G ED or AF-S NIKKOR 24–85 mm 1 : 3.5–4.5 G objectives.

Microscopy

Brightfield microscopy was performed using a Zeiss Axio Imager M2 upright microscope (Oberkochen, Germany) with EC Plan-Neofluar 10×/0.3, 20×/0.5 or 40×/0.75 objectives. Confocal laser scanning microscopy (CLSM) was performed on a Leica TCS SP8 with HC PL FLUOTAR (10×/0.30 dry) and HCX PL APO lambda blue (63×/1.20 water) objectives. Excitation and detection windows were set as follows: for visualization of lignin and cellulose: calcofluor (405 nm, 425–475 nm) and basic fuchsin (561 nm, 600–650 nm). Images were processed using Fiji software (Schindelin *et al.*, 2012). Scanning electronic microscopy was performed using a Zeiss Supra 40VP microscope.

Histochemistry

For toluidine blue staining, shoot apices, subterranean flowers and aerial and subterranean fruit at stages 17a and 17b were

fixed, embedded in LR White, sectioned, stained and imaged by light microscopy (Neumann & Hay, 2019). To visualize lignin by CLSM, 100–150 μm transverse sections were cut using a Leica Vibratome VT1000 S, immediately fixed and cleared using an adapted Clearsee protocol with Basic Fuchsin and Calcofluor white staining (Ursache *et al.*, 2018; Pérez Antón *et al.*, 2022). For SEM, plant material was fixed in 4% glutaraldehyde, dehydrated through an increasing ethanol series and critical point dried using a Leica CPD300 critical point dryer. Samples were mounted and sputter coated with platinum using a Polaron SC 7640 sputter coater.

High-speed video

Explosive pod shatter was filmed with a high-speed camera (Photron Fastcam SA3 120KM2; Photron Europe Ltd, Bucks, UK) fitted with a 100 mm F2.8 lens and recorded at 10 000 frames s^{-1} (Methods S1).

Time-lapse photography of subterranean fruit

Four-week-old *C. chenopodiifolia* plants were grown in a transparent chamber and roots and subterranean fruit were imaged every 30 min with a Canon EOS 700D camera equipped with an EF-S 18–55 mm f/3.5–5.6 lens (Methods S1).

Magnetic resonance imaging

MRI was performed at Jülich Forschungszentrum GmbH, Jülich, Germany, using a vertical bore 4.7 T magnet (Magnex, UK), on 10-wk-old plants grown in soil whose humidity was maintained constant at 70% of maximum water holding capacity (WHC_{max}; Pflugfelder *et al.*, 2022), image resolution: $0.3 \times 0.3 \times 0.6 \text{ mm}^3$; echo time: 9 ms, repetition time: 2 s and field of view: $77 \times 77 \times 84 \text{ mm}^3$.

RNA-seq analysis

RNA of aerial and subterranean fruit valves (stages 16–17a and 17ab) was extracted from three biological replicates using Spectrum™ Plant Total RNA kit (Sigma-Aldrich). Using the same method for RNA extraction, additional samples were harvested from nine different tissue types, three different hormone/elicitor treatments and light vs dark treatment of subterranean fruit valves. For long-read sequencing of all RNA samples, full-length complementary DNA (cDNA) synthesis was performed with TeloPrime Full-Length cDNA Amplification Kit (Lexogen; Cartolano *et al.*, 2016). Three single-molecule real-time (SMRT) bell libraries (Pacific Biosciences, Menlo Park, CA, USA) were prepared with the IsoSeq protocol and sequenced on PacBio Sequel II at the Max Planck Institute for Plant Breeding Research Genome Centre. PacBio IsoSeq data were demultiplexed and used to build a *C. chenopodiifolia* fruit reference transcriptome using SMRTLINK (v.10.2.0.133434), TAMA (tc_version_date_2019_11_19; Kuo *et al.*, 2020), MINIMAP2 (v.2.20-r1061; Li, 2018) and *C.*

chenopodiifolia genome assembly information (Emonet *et al.*, 2024). The transcriptome was annotated using TAMA and the UniRef90 database (Suzek *et al.*, 2007). For short-read sequencing of RNA from aerial and subterranean fruit valves (stage 16–17a and 17ab), the cDNA synthesis, Stranded Poly-A selection library preparation (two-sided, 150 bp) and sequencing were carried out by Novogene using the Illumina Nova-Seq6000 platform. Paired-end short reads were quality-checked, mapped to the *C. chenopodiifolia* reference transcriptome using default settings and quantified using SALMON (v1.8.0; Patro *et al.*, 2017). Differential expression analysis was performed with EDGER (v.3.42.4; Chen *et al.*, 2016). Cluster and Gene Ontology (GO) analyses were carried out using CLUSTERPROFILER (v.4.4.4; Wu *et al.*, 2021). GO annotations were retrieved by BLASTP (v.2.11.0+) using the *Arabidopsis thaliana* protein database (GCF_000001735.4) and complemented with GO terms retrieved from UniRef90. In addition, *C. chenopodiifolia* short reads were also mapped to the *C. hirsuta* genome (Gan *et al.*, 2016) and differential expression, GO and cluster analyses performed. For details, see Methods S1.

Statistical analysis

All statistical analyses were carried out using R (v.4.2.1) and RSTUDIO (v.2022.07.1; R Core Team, 2022).

Results

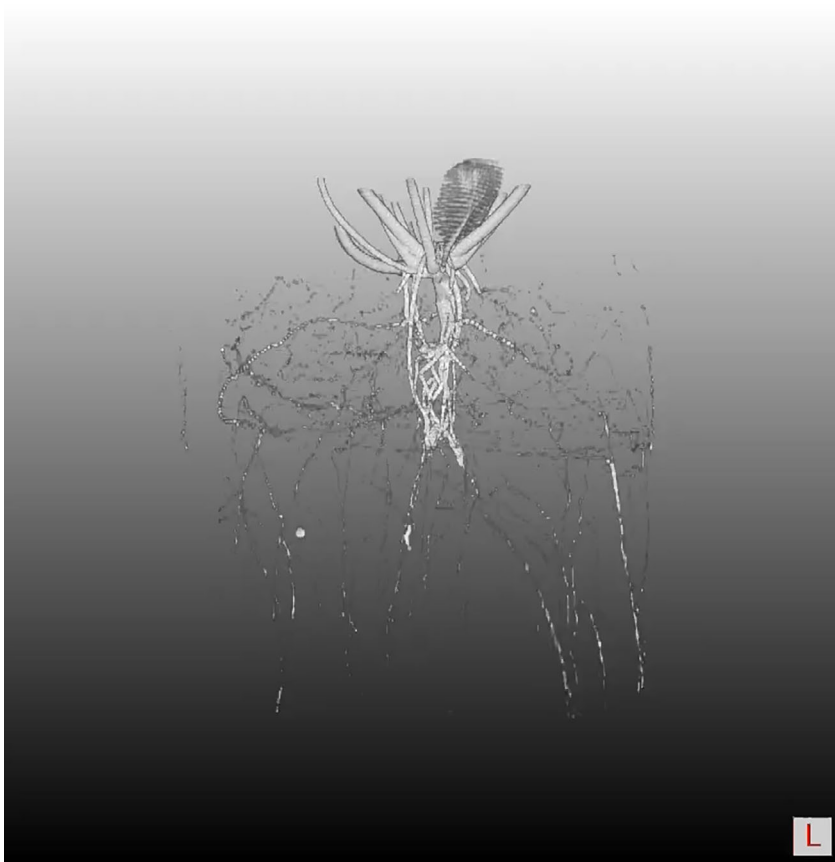
Amphicarpic: above- and belowground fruit

Two different types of fruit develop in *C. chenopodiifolia*: one type aboveground and the other belowground (Fig. 1a,e,f). *Cardamine chenopodiifolia* has a rosette flowering habit where the main shoot does not bolt (Fig. 1a–d). Subterranean fruit are derived from floral buds that develop at the inflorescence meristem on the main shoot (Fig. 1b–e). Each floral bud is immediately propelled into the soil by differential growth and rapid elongation of its pedicel (Fig. 1c; Video 1). When viewed from above, the pedicels extend downwards from the shoot apex, anchoring the rosette into the soil (Fig. 1d). Gravitropic growth of each pedicel continues underground to reach an average length of 5 cm (Fig. 1e,i). These pedicels have large cortical cells with Casparian strip-like lignin deposition in the innermost cortical cell layer surrounding the vasculature, which is absent in the pedicels of aerial fruit (Figs 1h, S1D). About 20 subterranean fruits develop in our standard growth conditions before termination of the inflorescence meristem (Fig. 1g). The first fruit produced usually grow close to the main root, while later fruit spread out around the periphery of the root system (imaged *in situ* by MRI, Video 2).

Aerial fruit, instead, are derived from flowers that develop on axillary shoots, which grow upwards away from gravity (Fig. 1a). These shoots form in the axils of rosette leaves. The rosette of *C. chenopodiifolia* generally comprises seven large, lobed leaves, arranged in a spiral phyllotaxy (Figs 1a,j, S1C,E). Soon after the transition to flowering, the growth of axillary meristems is released and five to six axillary shoots grow out (Figs 1d, S1A–C).



Video 1 Time-lapse photography of *Cardamine chenopodiifolia* subterranean fruit growing in soil over 26 d.



Video 2 Magnetic resonance imaging of *Cardamine chenopodiifolia* subterranean fruit growth in soil.

We found that flowering was accelerated in long-day compared with short-day photoperiods, indicating that *C. chenopodiifolia* is a long-day plant (Fig. 1k,l). In long-day conditions, floral buds were first visible at the main shoot apex 21 dpg and aerial flowers

were first observed on axillary shoots at 40 dpg (Fig. S1A,B). An average of 24 aerial fruits develop from the flowers on each shoot, excluding additional fruit that form on secondary branches (Fig. 1g).

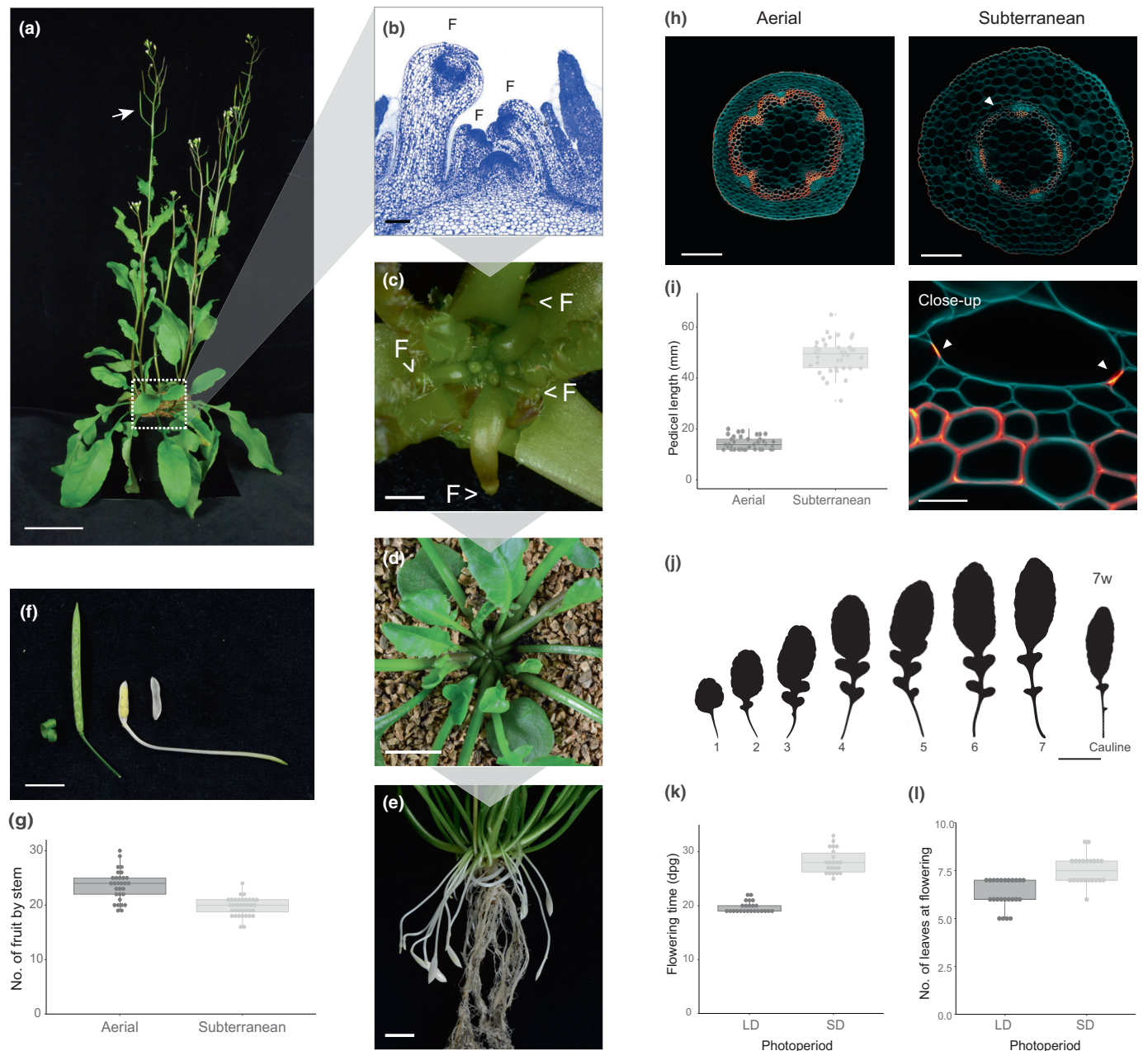
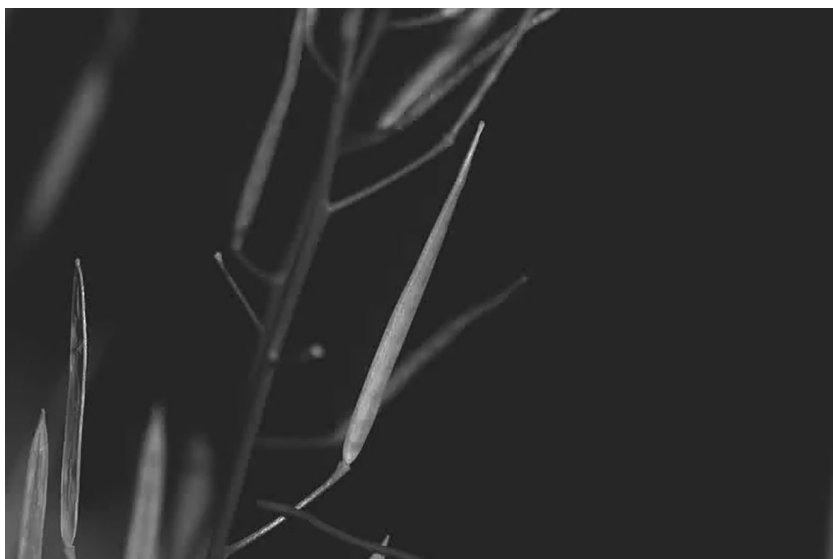


Fig. 1 *Cardamine chenopodiifolia* is amphicarpic. (a) *C. chenopodiifolia* plant at 60 d postgermination (dpg). Arrow indicates aerial fruit. Dashed box indicates position of main shoot apex. (b) Toluidine blue-stained longitudinal section through the inflorescence meristem of the main shoot apex. F, flower. (c) Top view of shoot apex of a 3-wk-old plant, with each floral bud propelled down into the soil by gravitropic growth of its pedicel. F, flower. (d) Top view of shoot apex of a 4-wk-old plant, with floral pedicels growing down into the soil and axillary shoots growing up out of the rosette. (e) Subterranean fruit and flowers borne on long pedicels, and roots, after soil removal from a 7-wk-old plant. (f) Aerial (left) and subterranean (right) fruit together with pedicels. Valve detached from aerial fruit coils explosively, while subterranean valve does not. (g) Box plot of number of fruit per stem in aerial and subterranean fruits. Plots show median (thick horizontal lines), $n = 30\text{--}40$ plants at c. 80 dpg. Differences between fruit morphs were analysed using the Wilcoxon test, $P = 1.111\text{e}\text{--}07$. (h) Confocal laser scanning micrographs of 100 μm transverse sections of aerial and subterranean pedicels stained with calcofluor white (cellulose, cyan) and basic fuchsin (lignin, Red Hot LUT). Localized lignin deposition in the innermost cortical cell layer surrounding the vasculature in subterranean pedicels, indicated by white arrowheads and in close-up view below. (i) Box plot of pedicel length in aerial and subterranean fruits. Plots show median (thick horizontal lines), $n = 30\text{--}40$ plants at c. 80 dpg. Differences between fruit morphs were analysed using the Wilcoxon test, $P = 2.711\text{e}\text{--}14$. (j) Heteroblastic series of rosette leaves and first cauline leaf in a 7-wk-old plant. (k, l) Box plots of flowering time, scored as the appearance of first floral bud at the main shoot apex (dpg) (k), and number of leaves at flowering time (l) for plants grown in long-day (LD) or short-day (SD) conditions. Plots show median (thick horizontal lines), $n = 24$ plants per photoperiod. Differences between photoperiods were analysed using the Wilcoxon test, $P = 3.811\text{e}\text{--}09$ (k), $P = 6.579\text{e}\text{--}06$ (l). Bars: 10 cm (a), 100 μm (b), 1 mm (c), 1 cm (d–f), 200 μm (h), 20 μm (close-up, h), 5 mm (j).



Video 3 High speed video of an exploding aerial fruit in *Cardamine chenopodiifolia* recorded at 10 000 frames per second.

Endocarp *b* lignification differs between fruit morphs

Both of the fruit morphs in *C. chenopodiifolia* are dehiscent siliques, but they employ different mechanisms of seed dispersal. Seeds are dispersed over a large area by explosive coiling of the two valves in aerial fruit (Video 3). The first aerial fruit explode after 11 wk of growth in long-day conditions (Fig. S1B). By contrast, subterranean fruit develop over a much longer period and dehisce nonexplosively to release their seeds underground long after all aerial fruit have exploded.

The two fruit morphs look very different: aerial fruit are elongated and green, while subterranean fruit are short and white (Figs 1f, 2a–c). Despite these differences, both fruit morphs elongate from stage 16 to 17a, then expand in girth during stage 17ab while the fruit tissues stiffen due to lignin deposition (Fig. 2a,f). Although these stages of fruit development are considerably longer in subterranean than aerial fruit, both fruit types reach their final size at stage 17b when the endocarp *b* is completely lignified (Fig. 2a–f). However, the last stages of development differ between the two morphs. Aerial fruit become yellow at stage 18 and have explosively released their seeds by stage 19, while subterranean fruit continue to develop and lignify through to stage 19, at which point they dry and dehisce to release their seeds (Fig. 2a,f).

Aerial fruit valves have a specific pattern of secondary cell wall lignification that is known to be critical in *C. hirsuta* for valves to explosively coil (Hofhuis *et al.*, 2016; Pérez Antón *et al.*, 2022). The valves of both *C. chenopodiifolia* fruit morphs comprise one exocarp cell layer, several layers of mesocarp cells and two endocarp cell layers, *a* and *b*, and it is these endocarp *b* cells that have a lignified secondary cell wall (Fig. 2d,e). In aerial fruit, the secondary cell wall is deposited only on the adaxial side of endocarp *b* cells (Fig. 2d–f). Lignin is deposited in a thin line that forms a ‘U’ in cross-section at stage 17ab of fruit development (Fig. 2f). By stage 17b, this lignified wall is very thick, but disrupted by two thin hinges at the base of the ‘U’ (Fig. 2f).

Subterranean fruit valves, instead, have one to three endocarp *b* cell layers with a uniform secondary cell wall pattern (Fig. 2d–f). Lignification initiates in cell corners at stage 17ab, but does not fill the apoplastic space between cells (Fig. 2f). Lignin deposition then continues throughout the cell wall, resulting in a uniformly thickened secondary cell wall by stage 17b (Fig. 2f). Multiple endocarp *b* cell layers can form in subterranean fruit valves, and although these cell layers are present in aerial fruit valves, they do not differentiate a lignified secondary cell wall (Fig. 2d,e). Therefore, the two fruit morphs differ not only in the initiation and patterning of endocarp *b* lignification, but also in the specification of endocarp *b* cell fate.

As subterranean fruit desiccate from stage 18 onwards, a small amount of lignin is deposited in mesocarp cell walls that are adjacent to endocarp *b* cells (Fig. 2f). Lignification of valve margin cells also begins at this stage in order to form a dehiscence zone between the replum and each valve (Figs 2b, S2A,B). In aerial fruit, by contrast, valve margin cells are fully lignified much earlier at stage 17b, when the lignification of endocarp *b* and replum cells is also completed (Figs 2b, S2A,B). Another conspicuous difference between the two fruit morphs is the sudden collapse of endocarp *a* cells between stages 17a and 17b in the valves of subterranean fruit, but not aerial fruit (Fig. 2d,e).

Seeds and flowers differ between fruit morphs

Seeds that develop in aerial vs subterranean fruit are distinguished by many characteristics related to their different modes of dispersal. Each aerial fruit contains *c.* 20 seeds compared with an average of only two seeds in subterranean fruit (Fig. 3a). These subterranean seeds are larger and heavier than aerial seeds (Fig. 3b–e). Aerial seeds are shaped like flattened discs compared with the more oval shape of subterranean seeds (Fig. 3b,f). Moreover, aerial seeds release a large amount of mucilage, compared with subterranean seeds, upon imbibition (Fig. 3g). This is reflected in a large difference in the amount of mucilage produced in epidermal cells of the seed coat in aerial compared with

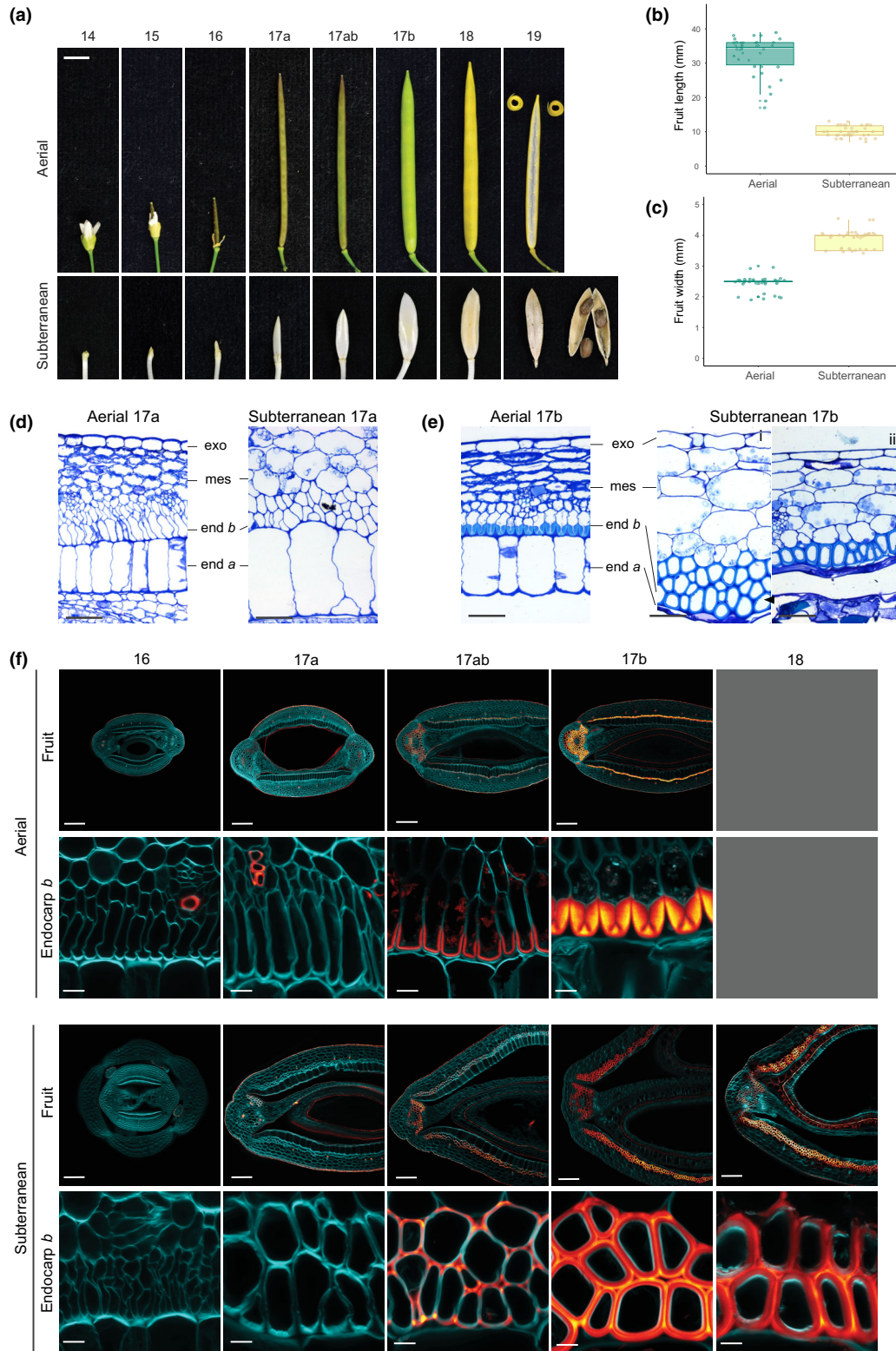


Fig. 2 Secondary cell wall patterning in endocarp *b* cells differs between aerial and subterranean fruit in *Cardamine chenopodiifolia*. (a) Aerial and subterranean flowers and fruit at stages 14 through 19. (b, c) Box plots of fruit length (b) and width (c) in aerial and subterranean fruits. Plots show median (thick horizontal lines), $n = 38\text{--}40$ fruit per morph. Differences between fruit morphs were analysed using the Wilcoxon test, $P = 5.558\text{e}\text{--}14$ (b) and $P = 4.214\text{e}\text{--}15$ (c). (d, e) Toluidine blue-stained transverse sections of aerial and subterranean fruit valves at stage 17a (d, before lignification) and 17b (e, after lignification). Lignin stains cyan. Exo, exocarp; mes, mesocarp; end *b*, endocarp *b*; end *a*, endocarp *a*. Arrows indicate endocarp *b* (e). (f) Confocal laser scanning micrographs of 100 μm transverse sections of aerial and subterranean fruit at stages 16 through 18 stained for cellulose (calcofluor white, cyan) and lignin (basic fuchsin, Red Hot LUT). Aerial fruit could not be sectioned at stage 18 due to explosive coiling. Bars: 5 mm (a) 50 μm (d, e), 100 μm (f, fruit) and 10 μm (f, endocarp *b*).

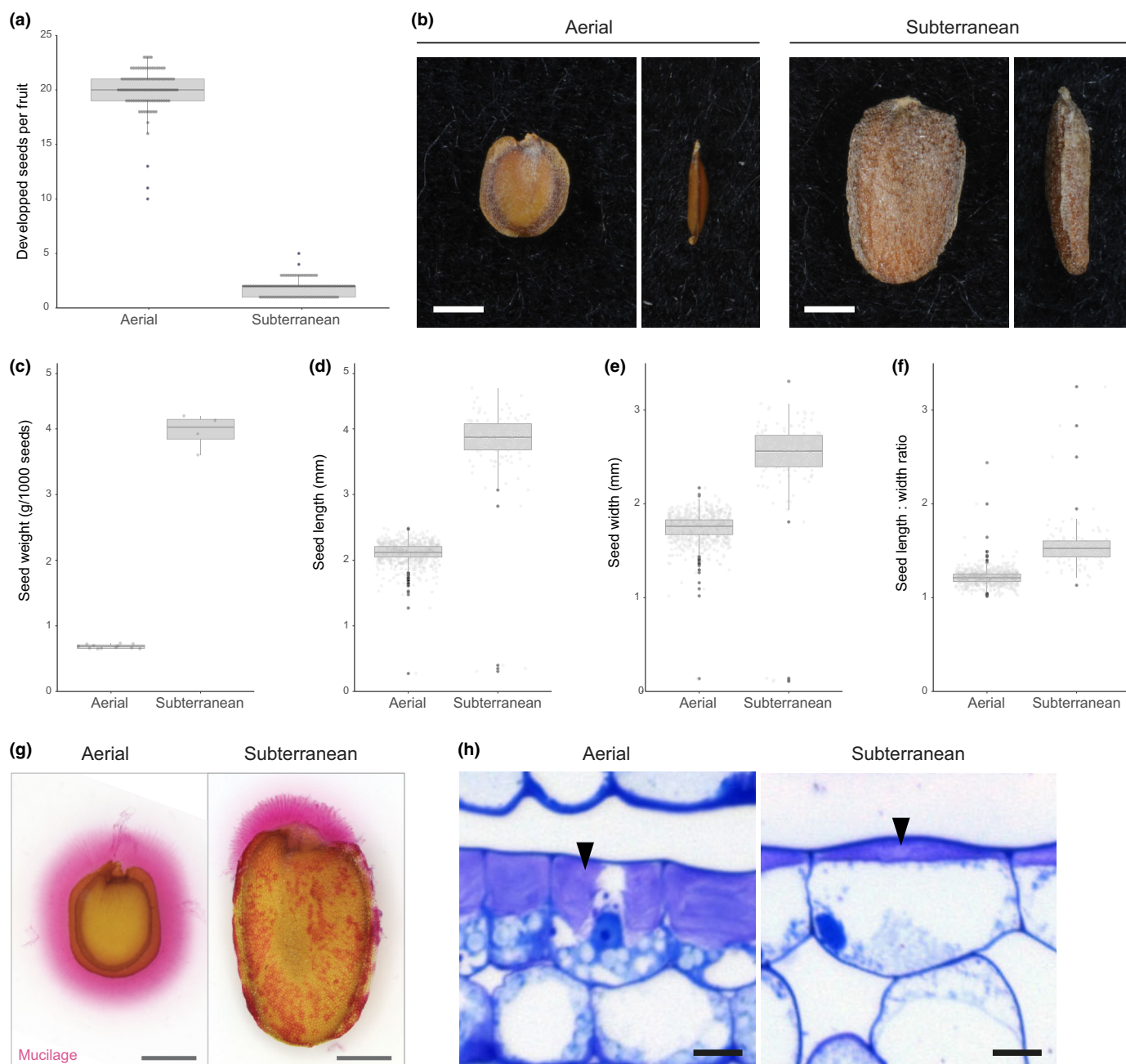


Fig. 3 Differences between aerial and subterranean seeds in *Cardamine chenopodiifolia*. (a) Box plot of seed number per fruit in aerial and subterranean fruits. Plot shows median (thick horizontal lines), $n = 100$ seeds per fruit type. Differences between fruit types were analysed using the Wilcoxon test, $P = 2e-16$. (b) Aerial and subterranean seeds shown from front (left) and side (right) views. (c–f) Box plots of seed weight per 1000 seeds (c), seed length (d), seed width (e) and seed length/width (f) in aerial and subterranean fruits. Plots show median (thick horizontal lines), $n = 115$ subterranean and 1970 aerial seeds from four plants. Differences between seed morphs were analysed using the Wilcoxon test, $P = 0.0011$ (c), $P < 2e-16$ (d–f). (g) Ruthenium red-stained mucilage (pink) released by aerial and subterranean seeds after imbibition. (h) Toluidine blue-stained transverse sections of outer seed coat of aerial and subterranean seeds from stage 17b fruit. Mucilage pockets indicated by black arrows. Bars: 1 mm (b, g), 10 μm (h).

subterranean seeds (Figs 3h, S2G). Other features, such as the seed coat surface and the seed abscission zone, appear very similar between both seed types (Fig. S2C–E). Therefore, aerial fruit produce numerous, small, mucilaginous seeds, suitable for long-range dispersal. By contrast, subterranean fruit produce few, large seeds, which is thought to aid germination from greater soil depths (Cheplick, 1987; Zhang *et al.*, 2020).

Both flower morphs in *C. chenopodiifolia* appear capable of self-pollinating. Selfing occurs in aerial flowers, which are typical of the Brassicaceae, with a perianth of four green sepals and four white petals, enclosing six stamens and two carpels (Fig. 4a,b). Subterranean flowers have the same number of floral organs as aerial flowers, but they are very reduced in size and sometimes fewer than four petals are observed (Figs 4a,c,

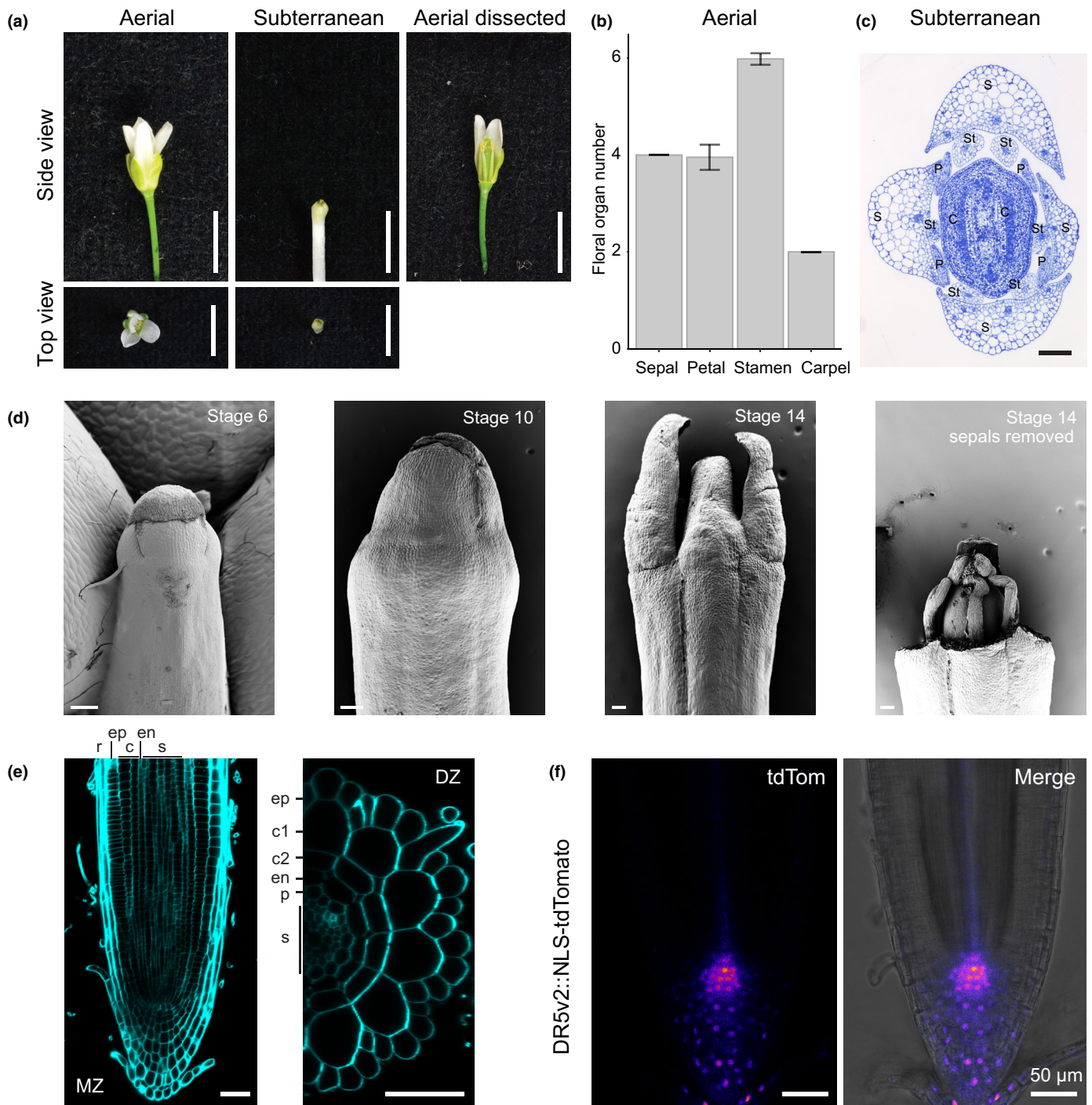


Fig. 4 Above- and belowground organs in *Cardamine chenopodiifolia*. (a) Aerial and subterranean flowers at stage 14, shown in side and top views. Perianth organs dissected off an aerial flower to show reproductive organs. (b) Bar plot of the number of sepals, petals, stamens and carpels in aerial flowers; plot shows mean and SD, $n = 87$. (c) Toluidine blue-stained transverse section of subterranean flowers at stage 14; C, carpels; P, petals; S, sepals; St, stamens. (d) Scanning electron micrographs of subterranean flowers at stages 6, 10 and 14; sepals dissected off a stage 14 flower to show reproductive organs. (e) Confocal laser scanning micrographs (CLSM) of seedling root tip meristematic zone (MZ, left) and optical section of root differentiation zone (DZ, right); c, cortex; c1, first cortex cell layer; c2, second cortex cell layer; en, endodermis; ep, epidermis; p, pericycle; r, root cap; s, stele. (f) CLSM of *DR5v2::NLS-tdTomato* expression (Fire LUT, left) and merged with brightfield image (right) in seedling root tip. Bars: 5 mm (a), 100 μ m (c, d), 50 μ m (e, f).

S2F). Subterranean flowers are nonopening and likely employ an automatic type of self-pollination called cleistogamy (Fig. 4a). The four sepals remain closed, protecting the

developing reproductive organs as the flower pushes through the soil (Video 1). Removing the sepals in stage 14 flowers reveals the pollen-bearing anthers in direct contact with the

stigmatic papillae of the gynaecium, suggesting that self-pollination occurs (Fig. 4d).

Roots of *C. chenopodiifolia* have a similar tissue structure to *C. hirsuta* (Hay *et al.*, 2014), comprising an epidermis, two cortex layers, an endodermis, a pericycle and vascular tissues filling the central cylinder (Fig. 4e). The quiescent centre is marked by a maximum of auxin activity, as reported by *DR5v2::NLS-tlTomato* (Fig. 4f). This transgene was stably transformed by floral dip of aerial flowers using *Agrobacterium tumefaciens* (see **Materials and Methods** section), demonstrating that transgenic approaches can be followed in *C. chenopodiifolia*.

In summary, *C. chenopodiifolia* is an amphicarpic plant that uses two very different strategies for seed dispersal. These strategies are associated with a suite of distinct traits that differentiate the development of reproductive structures above and below-ground. For these reasons, *C. chenopodiifolia* provides a unique framework to compare morphological divergence between two fruit morphs that develop on the same plant.

Comparative transcriptome analysis

To compare the transcriptome of aerial vs subterranean fruit valves in *C. chenopodiifolia*, we performed RNA-seq using both long-read

and short-read sequencing. We generated a reference transcriptome using Pacific Biosciences (PacBio) single-molecule real-time (SMRT) long-read isoform sequencing (IsoSeq; Fig. S3A). We took this approach since the polyploid *C. chenopodiifolia* genome was only recently assembled and not yet annotated or phased into sub-genomes (Emonet *et al.*, 2024). We sequenced RNA of aerial and subterranean fruit valves harvested at late stage 16 and stage 17ab, during which the valves grow to final length and endocarp *b* secondary cell walls start to lignify (Fig. 2). Developmental progression and onset of lignification during these stages are equivalent between fruit types (Fig. 2a,f). The four sample types were collected from the same plant, valves from five different plants were pooled to ensure sufficient material, and the experiment was performed in triplicate (Fig. 5a). To increase gene diversity, we sequenced additional samples harvested from nine different tissue types, three different hormone/elicitor treatments and light/ dark treatments of subterranean fruit valves (Methods S1). We collapsed all high-quality isoforms (Table S1) into a reference transcriptome containing 53 242 annotated genes.

To identify genes that are differentially regulated between aerial and subterranean fruit valves, and between different stages of fruit development, we used the same 12 RNA samples from *C. chenopodiifolia* valves for Illumina short-read sequencing (Fig. 5a;

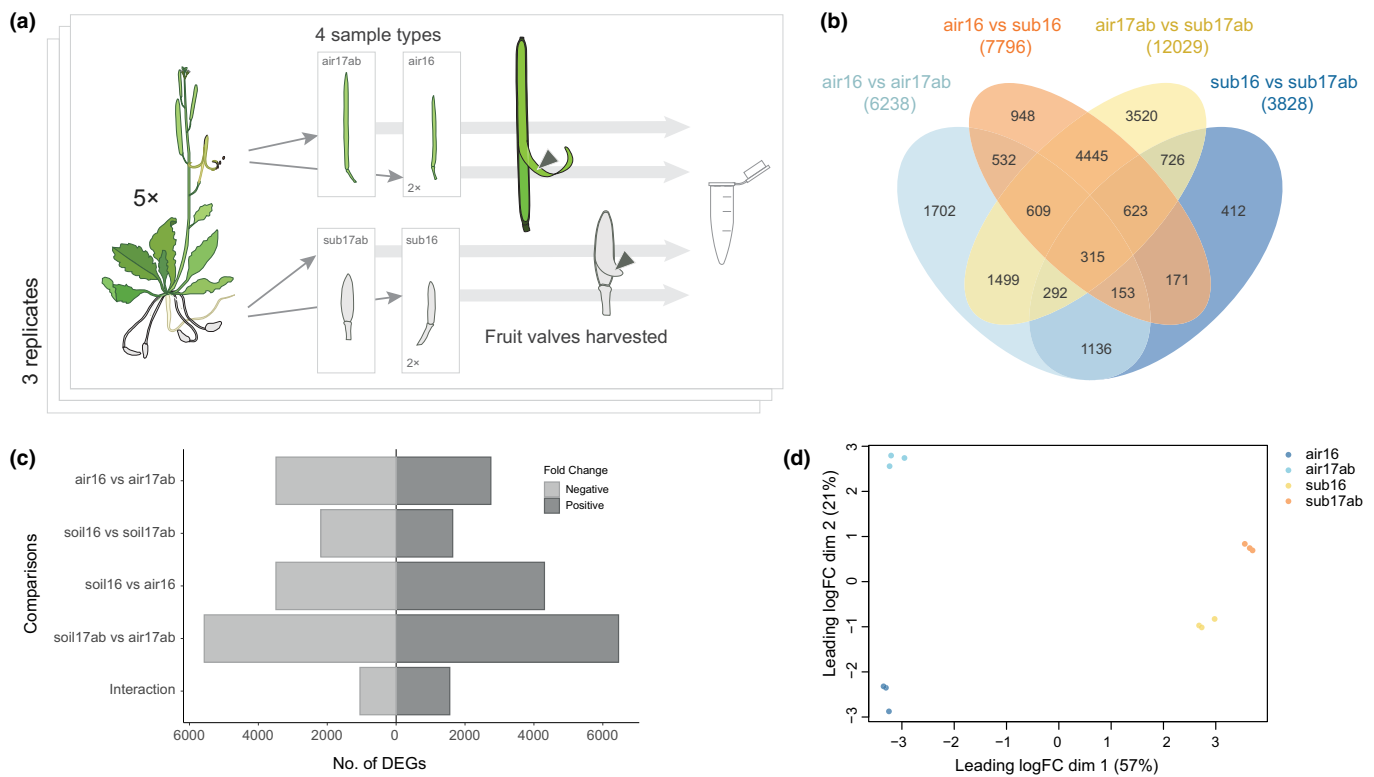


Fig. 5 Transcriptomes differ markedly between aerial and subterranean fruit valves in *Cardamine chenopodiifolia*. (a) Schematic of RNA-seq experimental design. (b) Venn diagram of differentially expressed genes (DEG, logFC ≥ |1|, false discovery rate (FDR) < 0.05) between aerial fruit stage 16 and aerial fruit stage 17ab (air16 and air17ab), aerial fruit stage 16 and subterranean fruit stage 16 (air16 and sub16), aerial fruit stage 17ab and subterranean fruit stage 17ab (air17ab and sub17ab), subterranean fruit stage 16 and subterranean fruit stage 17ab (sub16 and sub17ab). DEGs were obtained by mapping *C. chenopodiifolia* short reads to the *C. chenopodiifolia* reference transcriptome. (c) Number of up- and downregulated genes for each comparison (DEG, logFC ≥ |1|, FDR < 0.05). (d) Principal component analysis of short-read data from *C. chenopodiifolia* fruit valve sample types.

Table S2). We mapped these short reads to the *C. chenopodiifolia* reference transcriptome, which gave 46 411 genes with a Uniprot ID after low-count filtering (Table S1). We identified differentially expressed genes (DEGs) based on a false discovery rate (FDR) of < 0.05 and a minimum fold change of 2, for the four possible comparisons: aerial fruit stage 16 (air16) vs aerial fruit stage 17ab (air17ab), 6238 DEGs; subterranean fruit stage 16 (sub16) vs subterranean fruit stage 17ab (sub17ab), 3828 DEGs; air16 vs sub16, 7796 DEGs; air17ab vs sub17ab, 12 029 DEGs and 2607 DEGs from the interaction of both fruit stages and fruit types (Figs 5b,c, S3B–G; Tables S3, S4). We observed strong transcriptional changes for all comparisons, and in particular between the two fruit types at the later stage (17ab; Fig. 5b,c). Indeed, most of the variance between samples can be explained by the difference in fruit types (Fig. 5d). Many of the DEGs between fruit types were not differentially regulated across developmental stages (4445 DEGs; Fig. 5b). These genes might represent distinct responses to aerial vs subterranean environments, or could also generally distinguish the two fruit types. A larger number of DEGs were affected by developmental stage in aerial than in subterranean fruit, and more DEGs were upregulated than downregulated in aerial compared with subterranean fruit (Fig. 5c).

As an alternative approach, we also mapped the *C. chenopodiifolia* short reads to the high-quality, annotated, reference genome of the related diploid species *C. hirsuta* (Gan *et al.*, 2016; Fig. S3A). Only 18.6% of reads mapped to the *C. hirsuta* genome, aligning to 16 376 genes, with 11 870 genes in common to all four sample types, which corresponds to c. 40% of the annotated *C. hirsuta* genes (Fig. S4A; Table S3). Despite low mappability, the same dominant transcriptional trends were also found in this analysis (Figs S4, S5; Tables S3–S6).

Secondary cell wall formation is upregulated and cell division is downregulated during fruit valve development

One of the major events in both fruit types during the transition from stage 16 to 17ab is the deposition of a lignified secondary cell wall in the endocarp *b* cell layer of the valves. To assess whether our experimental design captured this, we performed GO analysis of common DEGs for these two comparisons (867 up- and 985 downregulated DEGs in stage 16 compared with stage 17ab, irrespective of fruit morph, Fig. 6a; Table S7). Enriched biological processes for upregulated genes included cell wall and secondary cell wall biogenesis, lignin/phenylpropanoid and xylan metabolic processes (Fig. 6b), suggesting that secondary cell wall formation dominates the processes occurring during these stages of valve development in both fruit types.

Both aerial and subterranean fruit have already elongated by stage 17ab (Fig. 1h), and this is reflected in the enrichment of GO terms related to cell division in downregulated genes (Fig. 6b). Enriched GO terms for the cell cycle, DNA replication, nuclear division, microtubule-based processes and spindle organization, support the idea that cell division is downregulated in stage 17ab fruit valves (Fig. 6b).

Subterranean fruit are characterized by defence responses and aerial fruit by photosynthesis

Growth in above- vs belowground environments will inevitably affect the transcriptome of these two *C. chenopodiifolia* fruit morphs. To investigate this, we analysed common DEGs between aerial and subterranean fruit independent of developmental stage (3502 up- and 2444 downregulated DEGs in aerial fruit compared with subterranean fruit, irrespective of stage, Fig. 6c). Subterranean fruit were characterized by enriched GO terms for innate immune response, systemic acquired resistance, and responses to ethylene, jasmonic acid, hypoxia and wounding (Fig. 6d; Table S7). Other enriched terms for plant defence included ‘killing of cells of another organism’, indole glucosinolate and camalexin biosynthesis (Fig. 6d). The abundance of microbiota in the soil likely explains why defence responses dominate the genes that are upregulated in subterranean fruit and downregulated in aerial fruit.

Photosynthesis was the most enriched biological process for genes upregulated in aerial fruit, and other enriched processes were all related to photosynthesis (Fig. 6d; Table S7). Therefore, photosynthetic processes dominate the transcriptional landscape of green aerial fruit, compared with white subterranean fruit, due to their exposure to light.

Distinct sets of primary and secondary cell wall-related genes and cytokinin responses are upregulated during the development of aerial fruit valves

To identify processes that distinguish the development of the two fruit types, we analysed interactions between fruit stage and type (INTX; Fig. S3B). To this end, we clustered the sequence reads of DEGs according to their behaviours across samples and performed GO analysis for three clusters with higher expression in aerial fruit (Clusters #2, #3 and #8, Fig. 7a,b; Table S8). Clusters #2 and #3 were enriched in genes related to cell wall processes (Fig. 7b; Table S8). Secondary cell wall processes, such as lignin/phenylpropanoid and glucuronoxylan biosynthesis, were specifically enriched in Cluster #3, while Cluster #2 contained GO terms related to the primary cell wall, such as pectin and xyloglucan biosynthesis (Fig. 7b). Another dominant process in Cluster #2 was response to cytokinin and cytokinin signalling pathways (Fig. 7b). Genes related to photosynthesis were over-represented in Cluster #8 and strongly downregulated during the development of subterranean fruit valves (Fig. 7a,b).

These results show that the upregulation of cell wall-related genes during fruit development distinguishes aerial from subterranean fruit valves, suggesting that distinct genes may be associated with the different patterns of lignified secondary cell walls in these two fruit morphs. To check that these genes (430 genes in Cluster #2 and 330 genes in Cluster #3; Fig. 7a,b) are distinct from those in common to both fruit types (867 genes; Fig. 6a), we compared both gene sets. Only 70 genes overlapped with Cluster #3 (Fig. 7d), characterized by enriched GO terms for secondary cell wall biogenesis (Table S9), and no genes overlapped with Cluster #2 (Fig. 7c). Therefore, the large majority of DEGs

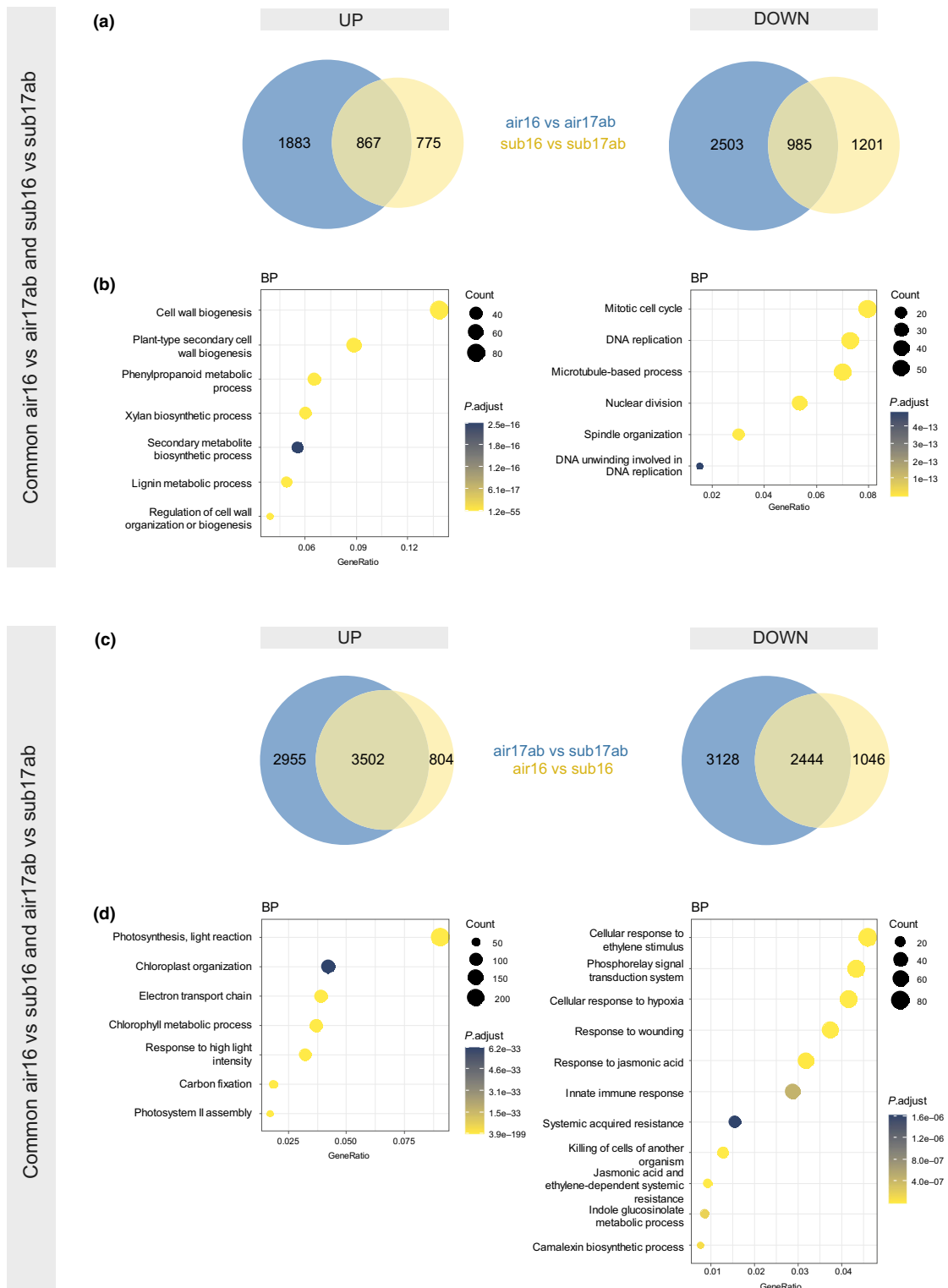


Fig. 6 Gene Ontology (GO) enrichments for differentially expressed genes (DEG) in common to fruit development or fruit type in *Cardamine chenopodiifolia*. (a) Venn diagrams of significantly up- and downregulated DEGs between stage 16 and stage 17ab aerial fruit compared with subterranean fruit ($\log_{FC} \geq |1|$, false discovery rate (FDR) < 0.05). (b) Selected GO terms enriched in the 867 upregulated DEGs and the 985 downregulated DEGs that are in common to both fruit types, and therefore distinguish the two stages of fruit development. (c) Venn diagrams of significantly up- and downregulated DEGs between aerial and subterranean fruit at stage 16 compared with stage 17ab ($\log_{FC} \geq |1|$, FDR < 0.05). (d) Selected GO terms enriched in the 3502 upregulated DEGs and the 2444 downregulated DEGs that are in common to both developmental stages, and therefore distinguish the two fruit types. DEGs were obtained by mapping *C. chenopodiifolia* short reads to the *C. chenopodiifolia* reference transcriptome. BP, biological process.

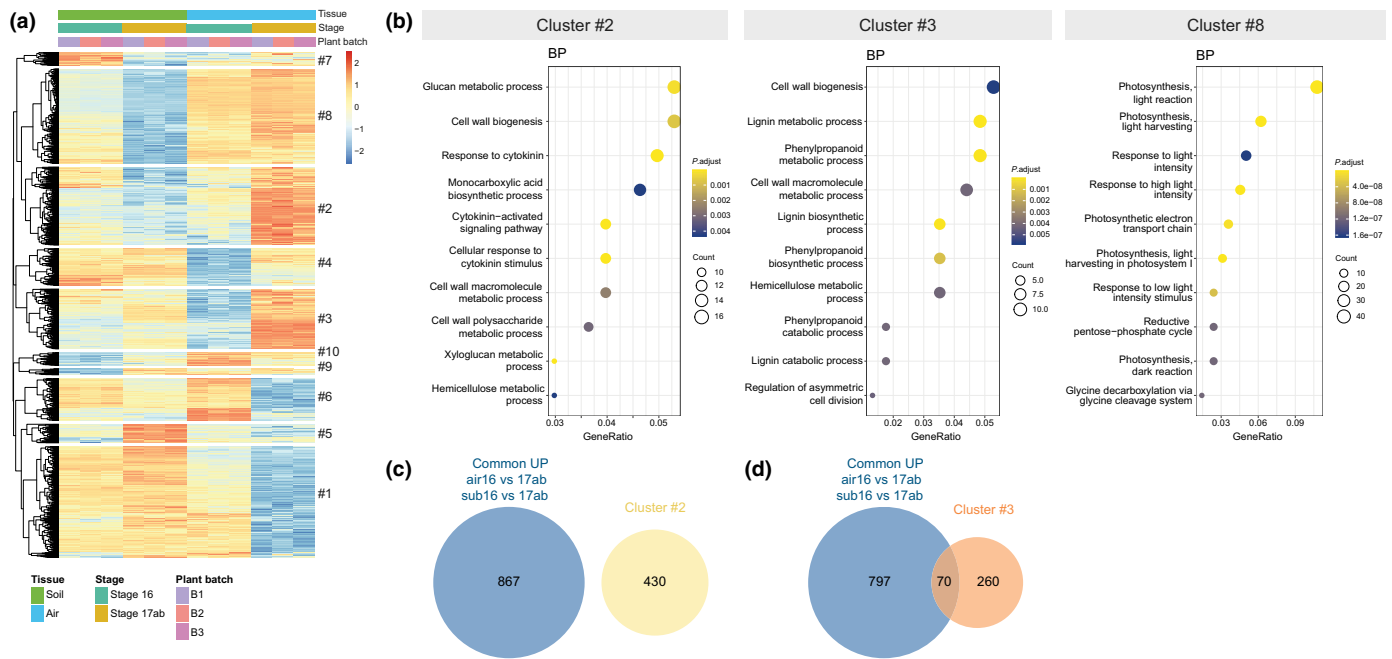


Fig. 7 Differentially expressed genes (DEG) that distinguish the development of different fruit types in *Cardamine chenopodiifolia*. (a) Heat map of significant DEGs for the interaction comparison (INTX) between fruit stage and type ($\log_{2}FC \geq |1|$, false discovery rate (FDR) < 0.05). DEGs were obtained by mapping *C. chenopodiifolia* short reads to the *C. chenopodiifolia* reference transcriptome. (b) Ten most significant Gene Ontology (GO) terms enriched in DEG Clusters #2, #3 and #8 from (a). (c, d) Venn diagram of 430 DEGs in INTX Cluster #2 (c) and 330 DEGs in INTX Cluster #3 (d) from (b), compared with 867 common DEGs upregulated in both aerial and subterranean fruit valves from Fig. 6(a).

in these clusters are specifically upregulated during the development of aerial fruit valves.

Discussion

Plant trait diversity is an important resource. Focusing on plants, such as *C. chenopodiifolia* that have not been well studied, opens up the possibility to understand the development and evolution of different traits and the diversity of mechanisms by which plants successfully adapt to different environments. We used morphological, histochemical and transcriptome approaches to characterize distinctive processes associated with amphicarpic development in *C. chenopodiifolia*. The tools generated in this study, together with a chromosome-level genome assembly (Emonet *et al.*, 2024), establish the allooctoploid *C. chenopodiifolia* as an emerging experimental system to address questions about polyploidy and trait evolution.

C. chenopodiifolia is an amphicarpic plant, producing two types of fruit on the same individual – above and belowground – with different seed dispersal strategies. Subterranean fruit are nonexplosive, dispersing seeds underground, and we found defence responses highly upregulated in these fruit valves that interface directly with the soil microbiome. Aerial fruit disperse seeds by explosive coiling of their two fruit valves, and we found a distinctive, polar pattern of secondary cell wall thickening in endocarp *b* cells of these valves. This matches the association between explosive seed dispersal and polar lignin deposition found previously in *Cardamine* (Hofhuis *et al.*, 2016). In stark contrast to this, the endocarp *b* cells in subterranean fruit valves

are uniformly lignified, similar to *Arabidopsis* and other Brassicaceae species with nonexplosive fruit (Spence *et al.*, 1996; Hofhuis *et al.*, 2016). Therefore, the uniform lignification of endocarp *b* cells is secondarily derived in the subterranean fruit of *C. chenopodiifolia*, together with nonexplosive seed dispersal.

Since the deposition of a thick, lignified secondary cell wall in endocarp *b* cells characterized valve development in both fruit types, it was not surprising to find that secondary cell wall processes dominated the DEGs upregulated in common to both fruit types. More surprising was that cell wall-related genes also distinguished the development of the two fruit types. Specifically, two of three large clusters that were strongly upregulated at late stages in aerial fruit valves, were enriched in genes related to cell wall processes (Fig. 7a,b). One of these clusters contained genes related to secondary cell wall formation (Cluster #3; Fig. 7b), and although 20% of these genes were in common to both fruit types, the majority were specifically upregulated in aerial fruit. Therefore, different genes are associated with the formation of lignified cell walls in the two different fruit morphs. Unexpectedly, the second cluster contained genes related to primary cell wall processes and cytokinin signalling (Cluster #2; Fig. 7b). Cytokinin is known to activate primary cell wall remodelling in the *Arabidopsis* root (Pacifi *et al.*, 2018). Whether cytokinin or primary cell wall pathways play any role in cell expansion or differentiation processes that are specific to explosive fruit are interesting questions for future research.

As a rare trait, amphicarpic provides unique insights into the development of very distinct reproductive structures in the above- vs belowground environment. Flowers produced by the

main shoot grow towards gravity and are well adapted to the soil environment. The strong and surprisingly long pedicels can dig the small flowers far below the surface and show circumnutation movements, which are known to help roots penetrate and grow around obstacles in the soil (Video 1; Taylor *et al.*, 2021). These pedicels also have Casparian strip-like lignin deposition and it will be interesting to understand whether this has a barrier function similar to the root (Naseer *et al.*, 2012). The underground flowers remain closed and are particularly reduced in size, as often seen in cleistogamous flowers. These characteristics might help to limit damage as the flowers progress through the soil. The soil environment also influences the transcriptome of these fruit valves, as genes involved in defence responses and innate immunity are upregulated. Roots are known to display a different immune response than the shoot in order to accommodate the soil microbiome (Wyrsh *et al.*, 2015; Poncini *et al.*, 2017). An interesting question to follow up is whether subterranean flowers and fruits are specifically adapted to the soil environment.

We described two types of flowering mode in *C. chenopodiifolia*: rosette flowering in the apical shoot, and inflorescence flowering in the axillary shoots. Plants such as *A. thaliana* and *C. hirsuta* transition to the reproductive phase through inflorescence flowering. By contrast, rosette flowering plants such as *Leavenworthia crassa* do not bolt, but instead, the main inflorescence produces flowers supported by long pedicels directly at the centre of the rosette (Liu *et al.*, 2011). *Cardamine chenopodiifolia* produces its subterranean flowers in a similar way, although the long pedicels are positively gravitropic and grow rapidly into the soil. The burial of cleistogamous flowers by elongating pedicels is a distinctive feature of *C. chenopodiifolia*. Cultivated peanut and some other amphicarpic plants rather bury fruit produced by the pollination of aerial flowers (Kumar *et al.*, 2019; Zhang *et al.*, 2020). Peanut is a geocarpic plant that develops only underground fruit, but a recently described variant also develops fruit aboveground (Peng *et al.*, 2024), and may prove useful for studying transitions between geocarpic and amphicarpic.

Stable genetic transformation in *C. chenopodiifolia* will be an essential tool to further investigate the many distinctive developmental processes associated with amphicarpic. We have provided a first proof of principle that Agrobacterium-mediated transformation by floral dip is possible, which paves the way for CRISPR/Cas9 gene editing and a suite of other molecular genetic approaches commonly used in model organisms. For example, the *DR5v2::NLS-tdTomato* transgenic line that we report here allows auxin-related processes, such as the gravitropic response of subterranean flowers, to be investigated in detail. The phylogenetic relatedness of *C. chenopodiifolia* to other model species in the Brassicaceae, such as *A. thaliana* and *C. hirsuta*, is also a distinct advantage for comparative studies. For example, inter-species gene transfers between related species are a powerful approach for functional studies of trait evolution (Hay & Tsiantis, 2006; Vlad *et al.*, 2014), particularly with CRISPR/Cas knock-in methods becoming more feasible (Schreiber *et al.*, 2024).

We showed that using long-read sequencing technologies, such as PacBio IsoSeq, to generate an accurate reference

transcriptome is a useful approach for polyploid species. In future studies, full annotation and phasing of the *C. chenopodiifolia* genome should help to link behaviour of the transcriptome with its sub-genomes. Polyploidy is a ubiquitous feature of plant genomes and often linked to trait evolution, yet natural polyploids are typically under-studied (Soltis & Soltis, 2016). Therefore, further development of the allooctoploid *C. chenopodiifolia* as a model system will provide important opportunities to advance the study of complex trait evolution by polyploidy.

Acknowledgements

We thank Peter Huijser for time-lapse photography, Rainer Franzen for scanning electron microscopy, Dagmar van Dusschoten and Daniel Pflugfelder for MRI measurements, Gregor Huber, Andreas Fischbach and Wolfram Faigl for their technical support and Hugo Hofhuis for preliminary observations. This work was supported by Swiss National Science Foundation fellowship P500PB_203021 to AE, RK acknowledges support from the Helmholtz Association for the Forschungszentrum Jülich GmbH. AH acknowledges support from a Max Planck Society core grant to the Department of Comparative Development and Genetics. Open Access funding enabled and organized by Projekt DEAL.

Competing interests

None declared.

Author contributions

AH and AE designed the research. AE, MPA and UN performed experiments. SD and AE analysed data. BH contributed PacBio sequencing and RK contributed Magnetic Resonance Imaging resources. AH and AE wrote the article. AH and AE acquired funding. AH supervised the research.

ORCID

Aurélia Emonet  <https://orcid.org/0000-0002-7682-655X>
 Angela Hay  <https://orcid.org/0000-0003-4609-5490>
 Bruno Huettel  <https://orcid.org/0000-0001-7165-1714>
 Robert Koller  <https://orcid.org/0000-0001-7251-7242>
 Ulla Neumann  <https://orcid.org/0000-0001-9200-4209>
 Miguel Pérez-Antón  <https://orcid.org/0000-0003-4071-7340>

Data availability

Short-sequence read data and PacBio long-sequence read data for this study have been deposited in the European Nucleotide Archive (ENA) at the European Molecular Biology Laboratory's European Bioinformatics Institute (EMBL-EBI) under accession no.: PRJEB69676 (<https://www.ebi.ac.uk/ena/browser/view/PRJEB69676>). The *C. chenopodiifolia* reference transcriptome and code for data analysis are available at Edmond, an open

research data repository of the Max Planck Society (doi: 10.17617/3.2JOOWA).

References

- Baumgarten L, Pieper B, Song B, Mane S, Lempe J, Lamb J, Cooke EL, Srivastava R, Strütt S, Žanko D *et al.* 2023. Pan-European study of genotypes and phenotypes in the Arabidopsis relative *Cardamine hirsuta* reveals how adaptation, demography, and development shape diversity patterns. *PLoS Biology* 21: e3002191.
- Bhatia N, Wilson-Sánchez D, Strauss S, Vuolo F, Pieper B, Hu Z, Rambaud-Lavigne L, Tsiantis M. 2023. Interspersed expression of CUP-SHAPED COTYLEDON2 and REDUCED COMPLEXITY shapes *Cardamine hirsuta* complex leaf form. *Current Biology* 33: 2977–2987.
- Cabrera AL. 1967. *Flora de la Provincia de Buenos Aires. Part III*. Buenos Aires, Argentina: Coleccion Cientifica Del I.N.T.A.
- Cartolano M, Huettel B, Hartwig B, Reinhardt R, Schneeberger K. 2016. cDNA library enrichment of full length transcripts for SMRT long read sequencing. *PLoS ONE* 11: e0157779.
- Chen Y, Lun ATL, Smyth GK. 2016. From reads to genes to pathways: differential expression analysis of RNA-Seq experiments using Rsubread and the edgeR quasi-likelihood pipeline. *F1000Research* 5: 1438.
- Cheplick G. 1983. Differences between plants arising from aerial and subterranean seeds in the Amphicarpic annual *Cardamine chenopodifolia* (Cruciferae). *Bulletin of the Torrey Botanical Club* 110: 442.
- Cheplick GP. 1987. The ecology of amphicarpic plants. *Trends in Ecology & Evolution* 2: 97–101.
- Clough SJ, Bent AF. 1998. Floral dip: a simplified method for *Agrobacterium*-mediated transformation of *Arabidopsis thaliana*. *The Plant Journal* 16: 735–743.
- Dinneny JR, Weigel D, Yanofsky MF. 2005. A genetic framework for fruit patterning in *Arabidopsis thaliana*. *Development* 132: 4687–4696.
- Emonet A, Awad M, Tikhomirov N, Vasilarou M, Perez-Anton M, Gan X, Novikova PY, Hay A. 2024. Polyploid genome assembly of *Cardamine chenopodiifolia*. *BioRxiv*. doi: 10.1101/2024.01.24.576990.
- Ferrández C, Liljegren SJ, Yanofsky MF. 2000. Negative regulation of the SHATTERPROOF genes by FRUITFULL during Arabidopsis fruit development. *Science* 289: 436–438.
- Gan X, Hay A, Kwantes M, Haberger G, Hallab A, Ioio RD, Hofhuis H, Pieper B, Cartolano M, Neumann U *et al.* 2016. The *Cardamine hirsuta* genome offers insight into the evolution of morphological diversity. *Nature Plants* 2: 1–7.
- Gianella M, Bradford KJ, Guzzon F. 2021. Ecological, (epi)genetic and physiological aspects of bet-hedging in angiosperms. *Plant Reproduction* 34: 21–36.
- Gorczyński T. 1930. Dalsze badania nad kleistogamją. II. *Cardamine chenopodifolia* Pers. [Continuation des recherches sur la cléistogamie. II. *Cardamine chenopodifolia* Pers.]. *Acta Societatis Botanicorum Poloniae* 7: 295–310.
- Hay A, Tsiantis M. 2006. The genetic basis for differences in leaf form between *Arabidopsis thaliana* and its wild relative *Cardamine hirsuta*. *Nature Genetics* 38: 942–947.
- Hay AS, Pieper B, Cooke E, Mandáková T, Cartolano M, Tattersall AD, Ioio RD, McGowan SJ, Barkoulas M, Galinha C *et al.* 2014. *Cardamine hirsuta*: a versatile genetic system for comparative studies. *The Plant Journal* 78: 1–15.
- Hofhuis H, Moulton D, Lessinnes T, Routier-Kierzkowska A-L, Bomphrey RJ, Mosca G, Reinhardt H, Sarchet P, Gan X, Tsiantis M *et al.* 2016. Morphomechanical innovation drives explosive seed dispersal. *Cell* 166: 222–233.
- Imbert E. 2002. Ecological consequences and ontogeny of seed heteromorphism. *Perspectives in Plant Ecology, Evolution and Systematics* 5: 13–36.
- Kaul V, Koul AK, Sharma MC. 2000. The underground flower. *Current Science* 78: 39–44.
- Kierzkowski D, Runions A, Vuolo F, Strauss S, Lymbouridou R, Routier-Kierzkowska A-L, Wilson-Sánchez D, Jenke H, Galinha C, Mosca G *et al.* 2019. A growth-based framework for leaf shape development and diversity. *Cell* 177: 1405–1418.e17.
- Kumar R, Pandey MK, Roychoudhry S, Nayyar H, Kepinski S, Varshney RK. 2019. Peg biology: deciphering the molecular regulations involved during peanut peg development. *Frontiers in Plant Science* 10: 1289.
- Kuo RI, Cheng Y, Zhang R, Brown JWS, Smith J, Archibald AL, Burt DW. 2020. Illuminating the dark side of the human transcriptome with long read transcript sequencing. *BMC Genomics* 21: 751.
- Lenser T, Graeber K, Cevik ÖS, Adigüzel N, Dönmez AA, Grosche C, Kettermann M, Mayland-Quellhorst S, Mérai Z, Mohammadin S *et al.* 2016. Developmental control and plasticity of fruit and seed dimorphism in *Aethionema arabicum*. *Plant Physiology* 172: 1691–1707.
- Li H. 2018. MINIMAP2: pairwise alignment for nucleotide sequences. *Bioinformatics* 34: 3094–3100.
- Liljegren SJ, Ditta GS, Eshed Y, Savidge B, Bowman JL, Yanofsky MF. 2000. SHATTERPROOF MADS-box genes control seed dispersal in Arabidopsis. *Nature* 404: 766–770.
- Liljegren SJ, Roeder AHK, Kempin SA, Gremiski K, Østergaard L, Guimil S, Reyes DK, Yanofsky MF. 2004. Control of fruit patterning in Arabidopsis by INDEHISCENT. *Cell* 116: 843–853.
- Liu N, Sliwinski MK, Correa R, Baum DA. 2011. Possible contributions of TERMINAL FLOWER 1 to the evolution of rosette flowering in *Leavenworthia* (Brassicaceae). *New Phytologist* 189: 616–628.
- Liu Y, Zhang X, Han K, Li R, Xu G, Han Y, Cui F, Fan S, Seim I, Fan G *et al.* 2021. Insights into amphicarpary from the compact genome of the legume *Amphicarpaea edgeworthii*. *Plant Biotechnology Journal* 19: 952–965.
- Lu J, Tan D, Baskin JM, Baskin CC. 2010. Fruit and seed heteromorphism in the cold desert annual ephemeral *Diptychocarpus strictus* (Brassicaceae) and possible adaptive significance. *Annals of Botany* 105: 999–1014.
- Lu JJ, Tan DY, Baskin JM, Baskin CC. 2015. Post-release fates of seeds in dehiscent and indehiscent siliques of the diaspore heteromorphic species *Diptychocarpus strictus* (Brassicaceae). *Perspectives in Plant Ecology, Evolution and Systematics* 17: 255–262.
- Manton I. 1932. Introduction to the general cytology of the Cruciferae. *Annals of Botany* 46: 509–556.
- McFarlane H, Gendre D, Western T. 2014. Seed coat ruthenium red staining assay. *Bio-Protocol* 4: e1096.
- Monniaux M, Pieper B, McKim SM, Routier-Kierzkowska A-L, Kierzkowski D, Smith RS, Hay A. 2018. The role of APETALA1 in petal number robustness. *eLife* 7: e39399.
- Naseer S, Lee Y, Lapierre C, Franke R, Nawrath C, Geldner N. 2012. Casparian strip diffusion barrier in Arabidopsis is made of a lignin polymer without suberin. *Proceedings of the National Academy of Sciences, USA* 109: 10101–10106.
- Neumann U, Hay A. 2019. Seed coat development in explosively dispersed seeds of *Cardamine hirsuta*. *Annals of Botany* 126: 39–59.
- Pacifici E, Di Mambro R, Dello Ioio R, Costantino P, Sabatini S. 2018. Acidic cell elongation drives cell differentiation in the Arabidopsis root. *EMBO Journal* 37: e99134.
- Patro R, Duggal G, Love MI, Irizarry RA, Kingsford C. 2017. Salmon provides fast and bias-aware quantification of transcript expression. *Nature Methods* 14: 417–419.
- Peng Z, Jia K-H, Meng J, Wang J, Zhang J, Li X, Wan S. 2024. Transcriptome profiling of aerial and subterranean peanut pod development. *Scientific Data* 11: 364.
- Pérez Antón M, Schneider I, Kroll P, Hofhuis H, Metzger S, Pauly M, Hay A. 2022. Explosive seed dispersal depends on SPL7 to ensure sufficient copper for localized lignin deposition via laccases. *Proceedings of the National Academy of Sciences, USA* 119: e2202287119.
- Persoon CH. 1807. *Synopsis plantarum, seu Enchiridium botanicum, complectens enumerationem systematicam specierum hucusque cognitarum*. Parisiis Lutetiorum, France: C.F. Cramerum.
- Pflugfelder D, Kochs J, Koller R, Jahnke S, Mohl C, Pariyar S, Fassbender H, Nagel KA, Watt M, van Dusschoten D. 2022. The root system architecture of wheat establishing in soil is associated with varying elongation rates of seminal roots: quantification using 4D magnetic resonance imaging. *Journal of Experimental Botany* 73: 2050–2060.
- Poncini L, Wyrsh I, Tendon VD, Vorley T, Boller T, Geldner N, Métraux J-P, Lehmann S. 2017. In roots of *Arabidopsis thaliana*, the damage-associated

molecular pattern AtPep1 is a stronger elicitor of immune signalling than flg22 or the chitin heptamer. *PLoS ONE* 12: e0185808.

- R Core Team. 2022. *R: a language and environment for statistical computing*. Vienna, Austria: R Foundation for Statistical Computing.
- Schindelin J, Arganda-Carreras I, Frise E, Kaynig V, Longair M, Pietzsch T, Preibisch S, Rueden C, Saalfeld S, Schmid B *et al.* 2012. Fiji: an open-source platform for biological-image analysis. *Nature Methods* 9: 676–682.
- Schreiber T, Prange A, Schäfer P, Iwen T, Grützner R, Marillonnet S, Lepage A, Javelle M, Paul W, Tissier A. 2024. Efficient scar-free knock-ins of several kilobases in plants by engineered CRISPR-Cas endonucleases. *Molecular Plant* 17: 824–837.
- Soltis DE, Visger CJ, Marchant DB, Soltis PS. 2016. Polyploidy: pitfalls and paths to a paradigm. *American Journal of Botany* 103: 1146–1166.
- Soltis PS, Soltis DE. 2016. Ancient WGD events as drivers of key innovations in angiosperms. *Current Opinion in Plant Biology* 30: 159–165.
- Spence J, Vercher Y, Gates P, Harris N. 1996. 'Pod shatter' in *Arabidopsis thaliana*, *Brassica napus* and *B. juncea*. *Journal of Microscopy* 181: 195–203.
- Suzek BE, Huang H, McGarvey P, Mazumder R, Wu CH. 2007. UniRef: comprehensive and non-redundant UniProt reference clusters. *Bioinformatics* 23: 1282–1288.
- Taylor I, Lehner K, McCaskey E, Nirmal N, Ozkan-Aydin Y, Murray-Cooper M, Jain R, Hawkes EW, Ronald PC, Goldman DI *et al.* 2021. Mechanism and function of root circumnutation. *Proceedings of the National Academy of Sciences, USA* 118: e2018940118.
- Ursache R, Andersen TG, Marhavý P, Geldner N. 2018. A protocol for combining fluorescent proteins with histological stains for diverse cell wall components. *The Plant Journal* 93: 399–412.
- Van de Peer Y, Ashman T-L, Soltis PS, Soltis DE. 2021. Polyploidy: an evolutionary and ecological force in stressful times. *Plant Cell* 33: 11–26.
- Van de Peer Y, Mizrahi E, Marchal K. 2017. The evolutionary significance of polyploidy. *Nature Reviews Genetics* 18: 411–424.
- Vlad D, Kierzkowski D, Rast MI, Vuolo F, Ioio RD, Galinha C, Gan X, Hajheidari M, Hay A, Smith RS *et al.* 2014. Leaf shape evolution through duplication, regulatory diversification, and loss of a homeobox gene. *Science* 343: 780–783.
- Wu T, Hu E, Xu S, Chen M, Guo P, Dai Z, Feng T, Zhou L, Tang W, Zhan L *et al.* 2021. CLUSTERPROFILER 4.0: a universal enrichment tool for interpreting omics data. *The Innovations* 2: 100141.
- Wyrsh I, Domínguez-Ferreras A, Geldner N, Boller T. 2015. Tissue-specific FLAGELLIN-SENSING 2 (FLS2) expression in roots restores immune responses in *Arabidopsis fls2* mutants. *New Phytologist* 206: 774–784.
- Zhang K, Baskin JM, Baskin CC, Cheplick GP, Yang X, Huang Z. 2020. Amphicarpic plants: definition, ecology, geographic distribution, systematics, life history, evolution and use in agriculture. *Biological Reviews* 95: 1442–1466.
- Zhuang W, Chen H, Yang M, Wang J, Pandey MK, Zhang C, Chang W-C, Zhang L, Zhang X, Tang R *et al.* 2019. The genome of cultivated peanut provides insight into legume karyotypes, polyploid evolution and crop domestication. *Nature Genetics* 51: 865–876.

Supporting Information

Additional Supporting Information may be found online in the Supporting Information section at the end of the article.

Fig. S1 Development and plant architecture of *Cardamine chenopodiifolia*.

Fig. S2 Aerial vs subterranean fruit and seeds in *Cardamine chenopodiifolia*.

Fig. S3 RNA-seq workflow and analysis using mapping of *Cardamine chenopodiifolia* short reads to the *C. chenopodiifolia* reference transcriptome.

Fig. S4 RNA-seq analysis using *Cardamine chenopodiifolia* short reads mapped to the *Cardamine hirsuta* genome.

Fig. S5 Gene Ontology (GO) enrichments for differentially expressed genes in common to fruit development or fruit type for alignment to *Cardamine hirsuta* genome.

Methods S1 Supplementary methods.

Table S1 *Cardamine chenopodiifolia* PacBio IsoSeq reference transcriptome statistics.

Table S2 *Cardamine chenopodiifolia* Illumina short-read statistics.

Table S3 Summary of differentially expressed genes in *Cardamine chenopodiifolia* fruit valves mapped to either the *C. chenopodiifolia* reference transcriptome or the *Cardamine hirsuta* genome.

Table S4 Differentially expressed gene list from *Cardamine chenopodiifolia* fruit valves using short reads mapped to the *C. chenopodiifolia* reference transcriptome.

Table S5 Differentially expressed gene list from *Cardamine chenopodiifolia* fruit valves using short reads mapped to the *Cardamine hirsuta* genome.

Table S6 Gene ontology analysis of differentially expressed genes in *Cardamine chenopodiifolia* fruit valves obtained from alignment to the *Cardamine hirsuta* genome (see Fig. S5).

Table S7 Gene ontology analysis of differentially expressed genes in *Cardamine chenopodiifolia* fruit valves obtained from alignment to the *C. chenopodiifolia* reference transcriptome (see Fig. 6).

Table S8 Gene ontology analysis of differentially expressed genes in the interaction between fruit stage and fruit type in *Cardamine chenopodiifolia* fruit valves.

Table S9 *Cardamine chenopodiifolia* gene list and associated gene ontology analysis for the intersection of genes in INTX cluster #3 with upregulated differentially expressed genes in common to both fruit types (see Fig. 7d).

Please note: Wiley is not responsible for the content or functionality of any Supporting Information supplied by the authors. Any queries (other than missing material) should be directed to the *New Phytologist* Central Office.